Dalton Transactions

ROYAL SOCIETY OF CHEMISTRY

PAPER

View Article Online
View Journal | View Issue

Check for updates

Cite this: *Dalton Trans.*, 2022, **51**, 12161

Introduction of a triphenylamine substituent on pyridyl rings as a springboard for a new appealing brightly luminescent 1,3-di-(2-pyridyl)benzene platinum(II) complex family†

Alessia Colombo, [a] Giulia De Soricellis,[a] Francesco Fagnani,[a] Claudia Dragonetti, *[a] Massimo Cocchi,[b] Bertrand Carboni, [c] Véronique Guerchais [c] and Daniele Marinotto [d]

Received 7th June 2022,
Accepted 18th July 2022

DOI: 10.1039/d2dt01792j

rsc.li/dalton

The preparation and characterization of three new complexes, namely [Pt(1,3-bis(4-triphenylamine-pyridin-2-yl)-4,6-difluoro-benzene)Cl] (**[PtL^{1}Cl]**), [Pt(1,3-bis(4-triphenylamine-pyridin-2-yl)-5-triphenylamine-benzene)Cl] (**[PtL^{2}Cl]**), and [Pt(1,3-bis(4-triphenylamine-pyridin-2-yl)-5-mesityl-benzene)Cl] (**[PtL^{3}Cl]**), is reported. All of them are highly luminescent in dilute deaerated dichloromethane solution (Φ_{lum} = 0.88–0.90, in the yellow-green region; the $\lambda_{max,em}$ in nm for the monomers are: 562, 561 and 549 for **[PtL^{1}Cl]**, **[PtL^{2}Cl]** and **[PtL^{3}Cl]**, respectively).**[PtL^{1}Cl]** is the most appealing, being characterized by a very long lifetime (103.9 μs) and displaying intense NIR emission in concentrated deaerated solution (Φ_{lum} = 0.66) with essentially no "contamination" by visible light < 600 nm. This complex allows the fabrication of both yellow-green and deep red/NIR OLEDs; OLED emissions are in the yellow-green (CIE = 0.38, 0.56) and deep red/NIR (CIE = 0.65, 0,34) regions, for **[PtL^{1}Cl]** 8 wt% (with 11% ph/e EQE) and pure **[PtL^{1}Cl]** (with 4.3% ph/e EQE), respectively.

1. Introduction

There is a growing interest in the study of square planar platinum(II) complexes for various applications like bioimaging,[1–8] electroluminescent devices,[9–21] sensing,[21–23] and nonlinear optics.[24–28] The significant spin–orbit coupling related to the platinum atom helps intersystem crossing, and consequently emission of light from triplet excited states, a performance that is further improved by the introduction of Pt–C bonds.[29–31] Because of this strong spin–orbit coupling, an internal electroluminescence quantum efficiency of one can be achieved in devices, since both the singlet and triplet excitons generated by electron–hole recombination (of which the ratio is 1 : 3) can be induced to emit (triplet harvesting).[32–34] For this reason, square planar platinum(II) complexes have become a centre of interest for the preparation of organic light-emitting diodes (OLEDs) which earned a pivotal position for solid-state lighting applications and full-color flat-panel display.[35,36] Due to their geometrical structure which favours the creation of aggregates or excimers by Pt–Pt or ligand–ligand intermolecular interactions,[20,37–42] they are a useful tool for the fabrication of deep-red to near infrared (NIR) OLEDs which have unique applications in optical communication, night-vision readable displays, and photodynamic therapy.[20,43–45] Moreover, platinum(II) aggregates, characterized by low-energy red to NIR emissions and by relatively long phosphorescence lifetimes, are especially attractive for application in biological imaging with the aim of improving the accuracy of medical diagnosis.[1–8] It is worth pointing out that finding red-emissive materials is a big challenge since the "energy gap law" predicts that the non-radiative decay rate constant increases exponentially with decreasing optical energy gap (ΔE_{opt}).[46]

In the last two decades it turned out that platinum(II) chlorido complexes with a cyclometalated terdentate 1,3-bis(pyridin-2-yl)benzene ligand (bpyb), which permits a rigid *N^C^N* coordination environment, are among the best emitters.[47–52] For example, in deaerated CH_2Cl_2, [Pt(bpyb)Cl] is characterized by an emission quantum yield (Φ_{lum}) of 0.60,[47] a value much larger than that observed for [Pt(*N^C*-2-

[a]*Dipartimento di Chimica, Università degli Studi di Milano, UdR INSTM di Milano, via C. Golgi 19, 20133 Milan, Italy. E-mail: claudia.dragonetti@unimi.it*
[b]*Istituto per la Sintesi Organica e la Fotoreattività (ISOF), Consiglio Nazionale delle Ricerche (CNR), via P. Gobetti 101, 40129 Bologna, Italy*
[c]*Université de Rennes 1, CNRS, ISCR (Institut des Sciences Chimiques de Rennes) – UMR 6226, F-35000 Rennes, France*
[d]*Istituto di Scienze e Tecnologie Chimiche (SCITEC) "Giulio Natta", Consiglio Nazionale delle Ricerche (CNR), via C. Golgi 19, 20133 Milan, Italy*

†Electronic supplementary information (ESI) available: Synthesis and characterization of the complexes, films preparation, and photoluminescence investigations. See DOI: https://doi.org/10.1039/d2dt01792j

phenylpyridine)(*N*-2-phenylpyridine)Cl] or the parent *N^N^C*-coordinated isomer.[49] Such a superiority has been attributed to the presence of the Pt–C bond, which causes a high ligand-field strength, and to the rigidity of the *N^C^N* ligand, which hinders distortions that would cause non-radiative decay.[49]

An appealing aspect of these platinum(II) chlorido compounds is that the introduction of suitable substituents, in the phenyl or pyridyl rings of the cyclometalated 1,3-bis(pyridin-2-yl) benzene ligand, allows to control the colour of the emission, keeping large quantum yields.[14] As a matter of fact, time-dependent density functional theory (TD-DFT) calculations put in evidence that the frontier orbitals are localised on diverse portions of the molecule, such that their energies can be altered practically independently.[53–55] Thus, in this kind of complexes in which the triplet state at lowest-energy has mainly HOMO → LUMO character, the phenyl ring makes the principal contribution to the HOMO whereas the pyridyl rings dominate in the LUMO. Accordingly, the introduction of electron-donating substituents in the phenyl ring (which raises the energy of the HOMO) and electron-accepting substituents in the pyridyl rings (which lowers the LUMO energy, especially in *para* of the N atoms) will allow to red-shift the emission, whereas electron-accepting substituents in the phenyl ring and electron-donating substituents in the pyridyl rings will lead to a blue-shift. The experimentally observed tendencies follow this design well.[3]

Thus, many derivatives of [Pt(1,3-bis(pyridin-2-yl)-5-R-benzene)Cl] (R = H) have been prepared and well characterized. For example, incorporation of an ester substituent at the 5 position of the central benzene ring leads to a blue-shift of the monomer emission (from 491 to 481 nm) whereas there is a progressive red-shift on going from R = mesityl (501 nm) to CH_3 (505 nm), tolyl (516 nm), thienyl (548) or dimethylaminophenyl (588 nm).[48] The study of the effect of the nature of the substituents at the 4 position of pyridyl rings has been mainly carried out with [Pt(1,3-bis(4-R-pyridin-2-yl)-4,6-difluoro-benzene)Cl] (R = H) as parent complex; as expected, there is a blue-shift of the monomer emission energy on going from R = CF_3 (496 nm)[15] to H (472 nm)[50] and NMe_2 (453 nm).[56] All these complexes are usually characterized by high quantum yields (Φ_{lum} = 0.50–0.87) and relative long lifetimes (τ = 5–10 μs).

In this context, we were curious to see the effect of the introduction of a polarizable π-delocalized bulky substituent on the phosphorescence properties of the [Pt(1,3-bis(pyridin-2-yl)-4,6-difluoro-benzene)Cl] complex. Therefore, we prepared the complex with a triphenylamine substituent at the 4 position of each pyridine **[PtL^{1}Cl]** (Scheme 1). This new complex is even more emissive than its known parent derivatives, in the yellow-green or deep red/NIR region depending on its concentration in solution. It is characterized by an unexpected long lifetime and can be used to prepare efficient yellow-green and deep red/NIR OLEDs. The related new complexes with a cyclometalated 5-triphenylamine-benzene **[PtL^{2}Cl]** or 5-mesityl-benzene **[PtL^{3}Cl]**, prepared for comparison, are also highly emissive leading to a new fascinating brightly luminescent family of cyclometalated 1,3-di-(2-pyridyl)benzene platinum(II) complexes.

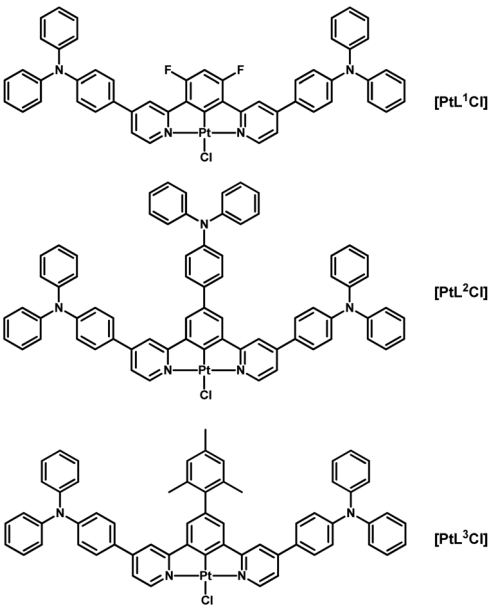

Scheme 1 Chemical structures of the investigated complexes.

2. Experimental

2.1 Synthesis of [PtL^{n}Cl]

The synthetic procedure is reported here. See details and full characterization in ESI.†

2.1.1 Procedure for the synthesis of pro-ligand HL^1. A two-necked round-bottom flask filled with argon was charged with 2-chloro-4-(triphenylamino)pyridine (**I1**, 1.35 mmol), 4,6-difluoro-1,3-phenyldiboronic acid pinacol ester (**I2**, 0.60 mmol, prepared as previously reported[56] by reaction of bis(pinacolato)diboron with 1,3-dibomo-4,6-difluorobenzene in the presence of Pd(dppf)Cl_2 and AcOK), 1,2-dimethoxyethane (8 mL), and a 1.2 M Na_2CO_3 solution (8 mL). The mixture was vigorously bubbled with argon for 30 min before adding $Pd(PPh_3)_4$ (0.1 mmol) and sealing the flask. The reaction mixture was heated at 100 °C for 24 h, and then cooled to room temperature. After addition of dichloromethane and water, the two layers were separated and the aqueous one was extracted twice with dichloromethane. The combined organic phases were washed with brine, dried over anhydrous $MgSO_4$ and concentrated *in vacuo*. The oily residue was purified by silica gel chromatography (eluent: cyclohexane/AcOEt, from 9 : 1 to 8 : 2) and a clear yellow lacquer was obtained (42% yield).

2.1.2 Procedure for the synthesis of complex [PtL^{1}Cl]. HL^1 (0.25 mmol) was solubilized in acetonitrile (12 mL) and placed under argon in a Schlenk tube. In parallel, K_2PtCl_4 (0.50 mmol) was dissolved in water (1.3 mL) using an ultrasonic bath and then added to the reaction vessel. The mixture was degassed by directly bubbling argon for 30 min in the solvent under stirring. The flask was then sealed and heated at 110 °C for three days. Upon cooling to room temperature, the suspension was filtered through a 0.45 μm Nylon membrane.

The isolated yellow solid was washed with water, diethyl ether and dried under vacuum (82% yield).

2.1.3 General procedure for the synthesis of pro-ligands HL^2 and HL^3. 2-Chloro-4-(triphenylamino)pyridine (**I1**, 3 mmol), 5-Ar-1,3-phenyldiboronic acid pinacol ester (1 mmol, Ar = triphenylamino for **I4** and Ar = mesityl for **I6**, both prepared as previously described in 2.1.1), Na_2CO_3 (7 mmol) and $Pd(PPh_3)_4$ (0.07 mmol) were added to a Schlenk tube together with 1,2-dimethoxyethane (1.5 mL) and water (1.5 mL). The reaction mixture was heated at reflux for 24 h under argon atmosphere. After cooling to room temperature, water and AcOEt were added and the phases were separated; the organic phase was washed with water, dried over Na_2SO_4 and evaporated at reduced pressure. The product was purified by flash chromatography on silica gel (eluent: hexane/AcOEt, 75/25 for HL^2 and 9/1 for HL^3), obtaining a white solid (55% yield for HL^2 and 57% for HL^3).

2.1.4 General procedure for the synthesis of complexes $[PtL^2Cl]$ and $[PtL^3Cl]$. HL^n (0.10 mmol) and K_2PtCl_4 (0.12 mmol) were added to a Schlenk tube, together with glacial AcOH (6 mL). The reaction mixture was heated at reflux under argon atmosphere. After 48 h, a precipitate had appeared and, once cooled to room temperature, water was added to precipitate all the product, which was filtered on a Buchner funnel and washed with water, methanol and diethyl ether, obtaining an orange powder (93% yield for $[PtL^3Cl]$ and 88% for $[PtL^3Cl]$).

2.2 Photophysical characterization

Electronic absorption spectra were obtained at room temperature in dichloromethane, by means of a Shimadzu UV3600 spectrophotometer and quartz cuvettes with 1 cm optical path length. Absolute photoluminescence quantum yields, Φ, were measured using a C11347 Quantaurus Hamamatsu Photonics K.K spectrometer, equipped with a 150 W Xenon lamp, an integrating sphere and a multichannel detector. Steady state and time-resolved fluorescence data were recorded with a FLS980 spectrofluorimeter (Edinburg Instrument Ltd). See details in ESI.†

2.3 Procedure for OLED fabrication with $[PtL^1Cl]$

OLEDs were fabricated by growing a sequence of thin layers on clean glass substrates pre-coated with a 120 nm-thick layer of indium tin oxide (ITO) with a sheet resistance of 20 U per square. A 2 nm-thick hole-injecting layer of MoOx was deposited on top of the ITO by thermal evaporation under high vacuum of 10^{-6} hPa. The other layers were deposited in succession by thermal evaporation under high vacuum: first, 4,4′,4″-tris(*N*-carbazolyl)triphenylamine (TCTA, 50 nm) as exciton blocking layers; second, the emitting layer (EML) evaporated by co-deposition of $[PtL^1Cl]$ and (bis-4-(*N*-carbazolyl)phenyl) phenylphosphine oxide (BCPO) to form a 30 nm-thick blend film (8 wt% Pt complex : 92 wt% BCPO), or by single deposition of the $[PtL^1Cl]$ complex only, to form a 30 nm neat film; third, 2,2′,2″-(1,3,5-benzinetriyl)-tris(1-phenyl-1-*H*-benzimidazole (TPBi, 30 nm) as an electron-transporting and hole-blocking layer. This was followed by thermal evaporation of the cathode layer consisting of 0.5 nm thick LiF and a 100 nm thick aluminium cap.

The current–voltage characteristics were measured with a Keithley Source-Measure unit, model 236, under continuous operation mode, while the light output power was measured with an EG&G power meter, and electroluminescence (EL) spectra recorded with a StellarNet spectroradiometer. All measurements were carried out at room temperature under argon atmosphere and were reproduced for many runs, excluding any irreversible chemical and morphological changes in the devices.

3. Results and discussion

3.1 Preparation of the new pro-ligands HL^n and related $[PtL^nCl]$ complexes

The new pro-ligands 1,3-bis(4-(triphenylamino)pyridin-2-yl)-4,6-diR_1-5-R_2-benzene (HL^1: R_1 = F, R_2 = H; HL^2: R_1 = H, R_2 = triphenylamino; HL^3: R_1 = H, R_2 = mesityl) were prepared by Suzuki–Miyaura cross-coupling of the corresponding boronic acid pinacol ester with 2-chloro-4-(triphenylamino)pyridine (see Scheme 2). Reaction of these pro-ligands with K_2PtCl_4 led to the desired $[PtL^nCl]$ complexes in 82–93% yields (see Experimental and ESI†).

3.2 Photophysical properties in solution and in solid state

The absorption spectra of $[PtL^1Cl]$, $[PtL^2Cl]$ and $[PtL^3Cl]$ complexes in dichloromethane solution at different concentrations are shown in Fig. 1 and relevant values are given in Table 1.

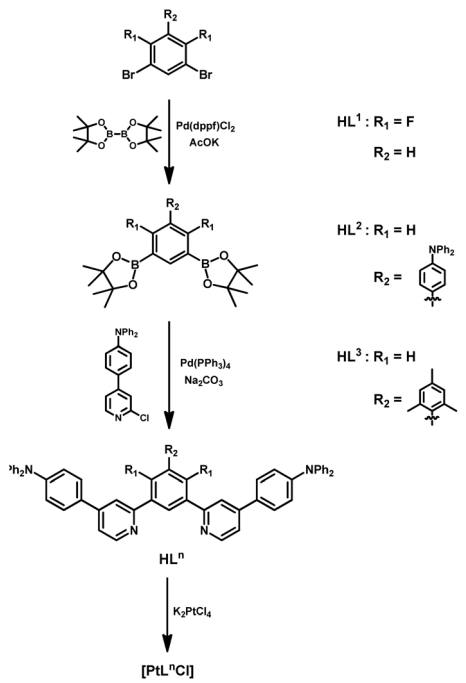

Scheme 2 Synthesis of $[PtL^nCl]$.

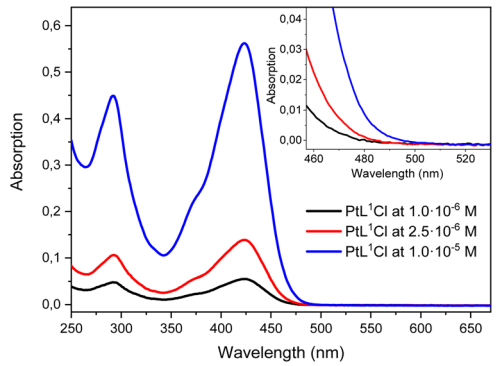

Fig. 1 Absorption spectra at different concentrations of **[PtL^{1}Cl]**, **[PtL^{2}Cl]** and **[PtL^{3}Cl]** in CH_2Cl_2 at 298 K. The weak bands at longer wavelengths are shown on an expanded scale for clarity.

Table 1 Photophysical parameters at 298 K in degassed CH_2Cl_2[a]

Complex	$\lambda_{max,abs}$/nm [ε/M^{-1} cm^{-1}]	$\lambda_{max,em}$/nm[b] Monomer [excimer/aggregate]	ϕ_{lum} Degassed [aerated]	τ/μs
[PtL^{1}Cl]	293 [4.5×10^4] 423 [5.6×10^4]	562 [696][c]	0.90 [0.059]	103.9
[PtL^{2}Cl]	296 [7.5×10^4] 425 [7.1×10^4] 502 [0.7×10^3]	561 [704][c]	0.88 [0.051]	6.6
[PtL^{3}Cl]	295 [5.9×10^4] 424 [8.0×10^4] 495 [1.0×10^3]	549 [727][c]	0.89 [<0.01]	50.0

[a] At 2×10^{-6} M. [b] Excitation at 422 nm. [c] Excimer and Aggregate at 2.4×10^{-4} M.

All three complexes show intense absorption bands at 260–320 nm which can be attributed to intraligand $^1\pi$–π^* transitions of the *N^C^N* ligand by analogy with related Pt(II) complexes;[57] moreover, intense bands are observed at around 350–470 nm which are attributed, by comparison with related cyclometalated Ir(III) complexes,[58] to an intraligand charge transfer (ILCT) from the triphenylamine moiety to the pyridyl rings; these strong latter bands cover the absorption bands (350–460 nm) of the charge-transfer transitions involving the cyclometalated ligand and the metal.[57] In addition, very weak absorption bands at lower energy (485–520 nm) are distinguishable in the absorption spectra of **[PtL^{2}Cl]** and **[PtL^{3}Cl]** complexes which are connected to direct population of $^3\pi$–π^* states facilitated by the high spin–orbit coupling associated with the Pt(II) center. Although a similar transition is also expected for the **[PtL^{1}Cl]** complex, no absorption band is detected up to 5×10^{-5} M, probably due to its low molar extinction coefficient (see Fig. S4 in ESI†).

Complexes **[PtL^{1}Cl]**, **[PtL^{2}Cl]** and **[PtL^{3}Cl]** are highly luminescent in dilute deaerated dichloromethane solution (2.5×10^{-6} M), with a luminescence quantum yield of 0.90, 0.88 and 0.89, respectively. **[PtL^{1}Cl]** displays a luminescence quantum yield which is similar or superior to that reported for the parent [Pt(1,3-bis(4-R-pyridin-2-yl)-4,6-difluoro-benzene)Cl] complexes with different R groups in *para* of the pyridine rings (Φ_{lum} = 0.80, 0.59, 0.87, 0.71, and 0.60, for R = H,[50] CF_3,[15] Me,[38] OMe[54] and NMe_2,[56] respectively). Besides, **[PtL^{3}Cl]** has a higher luminescence quantum yield than the related [Pt(1,3-bis(pyridin-2-yl)-mesityl-benzene)Cl] complex (Φ_{lum} = 0.62).[48]

The three complexes, at room temperature in dilute aerated dichloromethane solution, are very efficiently quenched by oxygen: the quantum yields of **[PtL^{1}Cl]**, **[PtL^{2}Cl]** and **[PtL^{3}Cl]** are 15, 17 and at least 89 times lower in air-equilibrated dichloromethane, respectively (Table 1); given the efficacy of oxygen quenching, efficient production of singlet oxygen – the $^1\Delta g$ state of O_2 – can be anticipated.

Upon excitation at around 422 nm, dilute dichloromethane solutions (1.0×10^{-6}–2.5×10^{-6} M) of complexes **[PtL^{1}Cl]**, **[PtL^{2}Cl]** and **[PtL^{3}Cl]** show intense phosphorescent bands in the yellow-green region with a maximum wavelength at 562, 561 and 549 nm (Fig. 2), respectively.

Thus, the substitution with the triphenylamine at the 4 position of each pyridine causes a strong red shift in the emission of complexes **[PtL^{1}Cl]** and **[PtL^{3}Cl]** with respect to the related [Pt(1,3-bis(4-R-pyridin-2-yl)-4,6-difluoro-benzene)Cl] (R = H) (472 nm)[50] and [Pt(1,3-bis(pyridin-2-yl)-5-R-benzene)Cl] (R = mesityl) (501 nm)[48] complexes, the strongest shift (90 nm) being observed for **[PtL^{1}Cl]**.

When the concentration of the **[PtL^{1}Cl]**, **[PtL^{2}Cl]** and **[PtL^{3}Cl]** complexes is increased up to around 2.4×10^{-4} M, new broad structureless emission bands arise at 696, 704 and 727 nm, respectively. These bands at lower energy can be ascribed to the emission from bi-molecular emissive excited states (excimers and aggregates) of the platinum(II) complexes, as previously reported.[52,57,59] Remarkably, the **[PtL^{1}Cl]** complex displays intense deep red/NIR emission (Φ_{lum} = 0.66) in concentrated deaerated solution with essentially no "contamination" by visible light < 600 nm. To our knowledge this represents the highest quantum yield in the deep red/NIR region reported for a platinum(II) complex in solution.

It is interesting to point out that an increase of the concentration of the three complexes doesn't lead to a strong decrease of the luminescence quantum yield in deareated dichloromethane solution (see Tables S1, S2 and S3 in the ESI†), in contrast to the behavior of other *N^C^N*-platinum(II) complexes.[52] Such a superior performance could be reasonably attributed to the presence of the sterically hindered triphenylamine substituents.

Lifetime measurements were performed on dilute deareated dichloromethane solutions at room temperature at the maximum emission wavelength of the **[PtL^{1}Cl]**, **[PtL^{2}Cl]** and **[PtL^{3}Cl]** complexes, exciting around 424 nm. Whereas **[PtL^{2}Cl]** has a lifetime (6.6 μs) in the typical range reported for *N^C^N*-platinum(II) complexes, **[PtL^{1}Cl]** and **[PtL^{3}Cl]** are characterized by an unexpected very long lifetime. Thus **[PtL^{1}Cl]** has a lifetime (103.9 μs) 16 times longer than that of the related [Pt(1,3-bis(pyridin-2-yl)-4,6-difluoro-benzene)Cl] complex (τ = 6.6 μs),[50] while the lifetime of **[PtL^{3}Cl]** (50.0 μs) is 7 times longer than that of [Pt(1,3-bis(pyridin-2-yl)-5-mesityl-benzene)Cl] (τ = 7.2 μs).[48]

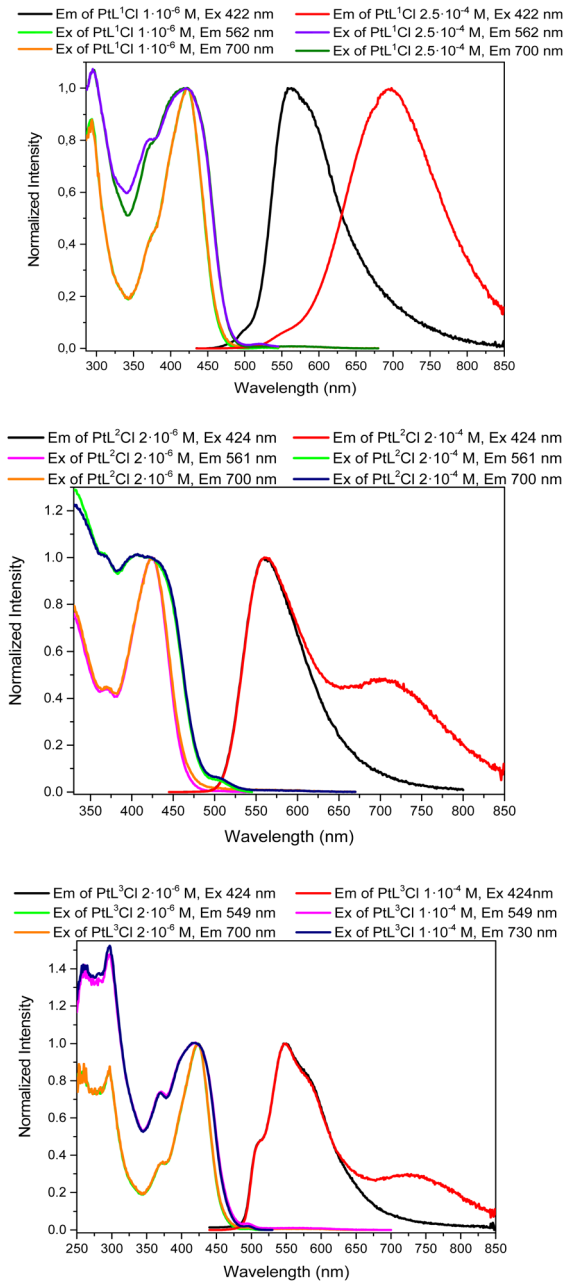

Fig. 2 Normalized emission and excitation spectra of diluted and concentrated solutions of **[PtL¹Cl]**, **[PtL²Cl]** and **[PtL³Cl]** in CH_2Cl_2 at 298 K.

The longer lifetimes of **[PtL¹Cl]** and **[PtL³Cl]** with respect to **[PtL²Cl]** can be associated to the structural variation of the substituent at the central aryl ring; in particular, we note that increasing the electron deficiency of the substituent (Ph_3N < mesityl < F2Ph) makes the lifetime of the complex longer. These large lifetimes are of particular relevance, being desirable for many applications such as bioimaging.[1–8]

Of the three new complexes analysed in solution at room temperature, **[PtL¹Cl]** is particularly appealing for its interesting photophysical properties such as high luminescent quantum yield, long lifetime and an emission that strongly depends on its concentration. Therefore, we decided to characterize the photophysical properties of the **[PtL¹Cl]** complex both in solution at low temperature (77 K, Fig. S15–S18†) and in the solid state as: blend in a polymethyl methacrylate (PMMA) matrix (0.5% w/w), neat thin film and powder; the preparation of the films can be found in the general information section of the ESI.† Table 2 reports the luminescence data for complex **[PtL¹Cl]** at the solid state.

The normalized emission and excitation spectra at 77 K of the **[PtL¹Cl]** complex at 2.4×10^{-4} M are shown in Fig. S15 (ESI†). The emission spectra of the **[PtL¹Cl]** display a structured phosphorescent band with a maximum wavelength at 546 nm (τ = 79.1 μs) and a broad structureless emission band at 684 nm (τ = 1.4 μs) which increases up to 730 nm (τ = 1.1 μs) by varying the excitation wavelength from 442 to 560 nm. The structured band is attributed to the monomers of the complex and, by comparison to the room temperature measurements (see Fig. S13†), it increases in intensity with respect to the broad structureless emission band at 684 nm. This behavior of the monomer signal is generally related to presence of excimers (emission at 684 nm); in fact, at low temperature the monomers have a reduced mobility and therefore a lower probability of excimer formation. The emission band at 730 nm is attributed to aggregates of the complex, as confirmed from the different excitation spectra recorded at 546 nm and 730 nm. It is interesting to note that the excitation spectrum at 546 nm and 684 nm are not equal in shape because the emission band at 730 nm partially overlaps to the excimer emission band.

The normalized absorption spectra of the neat and blend in PMMA thin films are shown in Fig. S19 (ESI†). The absorption spectrum of the thin film in PMMA is quite similar to that observed in solution. This is probably due to the weak intermolecular interactions felt by the **[PtL¹Cl]** molecules into the polymeric matrix. On the other hand, the neat film displays a broader absorption spectrum, due to the presence of excimers/aggregates.

The normalized emission and excitation spectra of the **[PtL¹Cl]** complex in PMMA film are given in Fig. S20 (ESI†). Upon excitation at 421 nm, the blend of **[PtL¹Cl]** in PMMA matrix shows intense phosphorescent bands with a maximum emission wavelength at 541 nm (τ = 35.0 μs), blue-shifted by *ca.* 21 nm with respect to the dilute dichloromethane solution. Moreover, a new band is observed at lower energy (*ca.*

Table 2 Photophysical parameters of various samples of **[PtL¹Cl]** at the solid state

Sample	$\lambda_{max,abs}$/nm	$\lambda_{max,em}$/nm	ϕ_{lum}	τ/μs
0.5% in PMMA	418	540, 570	0.56	34.95 20.85
Neat film	422	687	0.05	0.32
Powders at RT	—	653	0.11	0.56 [0.74][a]
Powders at LT	—	670	—	33.7 [0.99][a]

[a] Excimer/Aggregate.

670–740 nm) that increases by varying the excitation wavelength from 421 to 480 nm. This latter band can be ascribed mainly to the emission from aggregates of the **[PtL^{1}Cl]** complex, because of the limited mobility of the molecules into PMMA matrix, which prevents a high excimer formation. Furthermore, in support of this assignment, we note as the excitation spectra recorded at 541 nm and 700 nm are different in shape.

The normalized emission and excitation spectra of **[PtL^{1}Cl]** as neat film are given in Fig. S23 (ESI†). Regardless of the excitation wavelength, the neat film shows only one phosphorescent band with a maximum emission wavelength at 688 nm. The spectral position of this band is similar to that observed in solution at 2.5×10^{-4} M at room and low temperature (see Fig. 2 and S15), therefore, it can be ascribed to the emission from bi-molecular emissive excited states (excimers and aggregates) of the **[PtL^{1}Cl]** complex. Moreover, lifetime measurements performed at 691 nm, exciting at 404 nm, show two values: τ_1 = 94.71 ns and τ_2 = 342.27 ns (see ESI†).

The normalized emission and excitation spectra of the powder of the **[PtL^{1}Cl]** complex at room temperature and 77 K are shown in Fig. S25 and S29 (ESI†), respectively. The emission spectra at room temperature are characterized by a broad structureless band at 652 nm (τ = 0.74 μs) with shoulders at 535 (τ = 0.56 μs) and 580 nm (τ = 0.87 μs) that decrease in intensity by varying the excitation wavelength from 460 to 500 nm.

At 77 K, the emission spectra of the powder shown a more intense structured band at 552 nm (τ = 33.7 μs) and a structureless band at 667 nm (τ = 0.99 μs), which is red-shifted by *ca.* 15 nm with respect to the powder at room temperature, (see Fig. 3). The peaks at 552 and 580 nm can be attributed to the monomer excitonic states of the complex by comparison to the emission spectra of the **[PtL^{1}Cl]** in PMMA film (see Fig. 3). Interestingly, the emission spectra have a very similar behavior to these observed for a concentrated solution (2.4×10^{-4} M) at 77 K (see Fig. S33, ESI†); therefore, it is reasonable to assume that peak at 667 nm is mainly composed by excimer emission. However, since the excitation spectra at 552 nm and 667 nm are different from each other, it is not possible to exclude the presence of aggregates.

The luminescent quantum yield of the neat and PMMA thin film is 0.05 and 0.56, respectively, while is 0.11 for the powder. Clearly, although a significant quantum yield is maintained in the PMMA film, the higher presence of excimers and aggregates in the neat film and powder causes a strong quenching of the quantum yield.

3.3 Fabrication of OLEDs based on [PtL^{1}Cl]

Highly luminescent platinum(II) chlorido complexes with a cyclometalated 1,3-di(2-pyridyl)benzene ligand have been used as emitters in multilayer OLEDs, affording high external quantum efficiencies.[16] They showed their great potential for tailoring the emission colour of OLEDs. As a matter of fact, they are characterized by two phosphorescence bands, located in the bluish green (monomeric emission) and red (excimer/aggregate emission) regions of the visible spectrum, which contributions to the total emission can be controlled by the concentration of the platinum complex in the host matrix used for the fabrication of the blend emissive layer of the OLED. Thus, it was reported that [Pt(1,3-bis(pyridin-2-yl)-4,6-difluorobenzene)Cl] allows the preparation of bluish green (5 wt% of

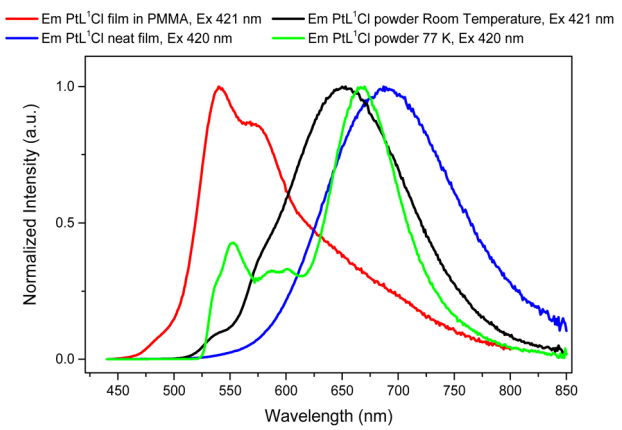

Fig. 3 Normalized emission spectra of **[PtL^{1}Cl]** complex in solid state.

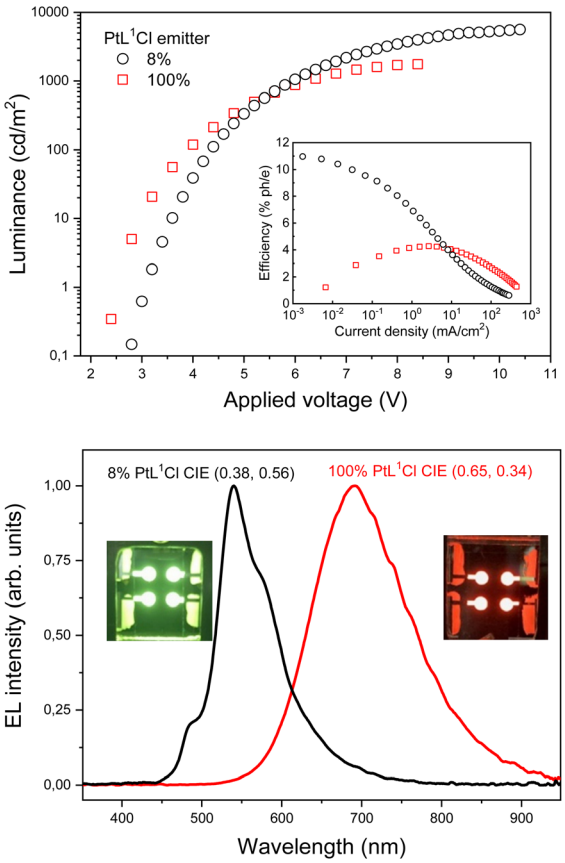

Fig. 4 (a) Luminance *vs.* applied voltage and external EL efficiency *vs.* current density (inset) of the OLEDs. (b) Electroluminescence spectra at 7 V of OLEDs. In the inset there are photos of yellow-green and deep red OLEDs based on **[PtL^{1}Cl]**.

Table 3 Optoelectronic performance of the OLEDs tested

		Maximum elettroluminescence efficiencies @max @100 cd m^{-2} @1000 cd m^{-2}			Maximum elettroluminescence intensity		Color paramiters		
PtL^1 Cl	Turn-on voltage (V)	EQE (%ph/e)	Current efficiency (cd/A)	Power efficiency (lm/W)	B (cd m^{-2})	P (mW cm^{-2})	CIE (x;y)	Dominat wavelength (nm) purity (%)	CCT (°K)
8%	3.0	11.0	35.5	37.3	5610	3.8	(0.38;0.56)	563	5860
		8.1	26.0	18.6				84	
		4.0	12.9	6.8					
100%	2.6	4.3	1.3	1.4	1750	10.0	(0.65;0.34)	607	1000
		4.1	1.3	1.0				99	
		2.5	0.8	0.4					

complex in the emitting layer) and red (100 wt% of complex) OLEDs, the introduction of CH_3 groups in *para* of the pyridine rings leading to better quantum efficiencies.[38]

Substitution of the methyl groups with electron-donating dimethylamino substituents causes a blue-shift of the monomer emission, allowing the preparation of blue (3–5 wt% complex within the emitting layer), white (20 wt%) and amber (100 wt%) OLEDs.[56] Similar results were obtained with less donor methoxy groups in *para* of the pyridines[54] whereas the use of electron-withdrawing CF_3 groups allows to prepare green-yellow OLEDs, at the concentration of 5 wt% in the emitting layer, and deep red OLEDS, when used as neat-film emitter.[15]

In the present work, OLEDs were fabricated using as emitting layer either a matrix of BCPO matrix hosting the **[PtL^{1}Cl]** complex (8 wt%) or a film of pure **[PtL^{1}Cl]**. Holes were injected from the indium tin oxide anode and passed through a 50 nm thick transporting layer made of 4,4′,4″-tris(*N*-carbazolyl)triphenylamine TCTA.

Electrons were injected from an Al/LiF cathode and transported to the emitting layer (EML) by means of a layer of 2,2′,2″-(1,3,5-benzinetriyl)-tris(1-phenyl-1-*H*-benzimidazole) (TPBi, 30 nm thick). Charges recombined in the 30 nm thick EML made of pure **[PtL^{1}Cl]** or of a BCPO matrix hosting the **[PtL^{1}Cl]** (8 wt%). EL spectra of the OLEDs are shown in Fig. 4. OLED emissions are in the yellow-green (CIE = 0.38, 0.56) and deep red (CIE = 0.65, 0.34) regions, for **[PtL^{1}Cl]** 8 wt% and pure **[PtL^{1}Cl]**, respectively.

There is no substantial contribution to the EL emission bands from the electron-transporting (hole-blocking) or TCTA binder layers, in accordance with a good charge carrier confinement within the EML and complete energy transfer from the excited states of BCPO (formed by charge carrier recombination) to the Pt complex.

The luminance and external EL efficiency as function of current density and applied voltage of both OLEDs are shown in Fig. 4a. The EL efficiency shows the typical roll-off at high currents due to exciton–exciton and/or exciton/charge interaction and to high field induced exciton dissociation.[60] Nevertheless, for **[PtL^{1}Cl]** pure film as EML the efficiency remains in excess of 1.5% for all range of current density while EL efficiency drops off an order of magnitude when **[PtL^{1}Cl]** has been employed as the emitting dopants (inset of Fig. 4a). Clearly, the shorter luminescence lifetime of aggregate **[PtL^{1}Cl]** (high concentration) compared to **[PtL^{1}Cl]** monomer (low concentration) ensures that there is a lower probability of the excited state being quenched. Although the maximum brightness of 1750 cd m^{-2} achieved for **[PtL^{1}Cl]** pure film as EML is apparently less than the value of 5610 cd m^{-2} for **[PtL^{1}Cl]** as dopant in BCPO (see Table 3), it should be noted that this is a photometric (as opposed to radiometric) measurement of brightness factors in the eye's sensitivity, which falls to zero beyond 700 nm. In fact, EL intensity of OLED based on **[PtL^{1}Cl]** pure film reaches 10 mW cm^{-2}, a good result compared to the best deep red/NIR OLEDs (see Table 3).[61–65]

4. Conclusion

In conclusion, a new brightly luminescent family of 1,3-di-(2-pyridyl)benzene platinum(II) complexes bearing a triphenylamine substituent on the pyridyl rings has been discovered. It was shown how the color of the phosphorecence can be tuned by the nature of the substituents on the benzene ring, keeping quantum yields near unity thanks to the presence of the triphenylamine substituents on the pyridines. The novel [Pt(1,3-bis(4-triphenylamine-pyridin-2-yl)-4,6-difluoro-benzene)Cl] complex is particularly fascinating: in diluted deaerated solution it displays intense yellow-green emission (Φ_{lum} = 0.90) with an unexpected very long lifetime (103.9 μs) whereas in concentrated deaerated solution it displays intense deep red/NIR emission (Φ_{lum} = 0.66) with essentially no "contamination" by visible light < 600 nm. To our knowledge this represents the highest quantum yield in the deep red/NIR region reported for a platinum(II) complex in solution. Thus, our new complex, which allowed the preparation of efficient yellow-green and deep red/NIR OLEDs, represents surely a useful tool for bio-imaging.

Conflicts of interest

There are no conflicts to declare.

Acknowledgements

We deeply thank Prof. Dominique Roberto for fruitful discussions. The National Interuniversity Consortium of Materials Science and Technology (PROGETTO INSTM21MIROBERTO), the Università degli Studi di Milano (PSR2020_DIP_005_PI_ACOLO), CNR are acknowledged for financial support in Italy.

Notes and references

1 V. Fernandez-Moreira, F. L. Thorp-Greenwood and M. P. Coogan, *Chem. Commun.*, 2010, **46**, 186–202.
2 Q. Zhao, C. Huang and F. Li, *Chem. Soc. Rev.*, 2011, **40**, 2508–2524.
3 E. Baggaley, J. A. Weinstein and J. A. G. Williams, *Coord. Chem. Rev.*, 2012, **256**, 1762–1785.
4 E. Baggaley, S. W. Botchway, J. W. Haycock, H. Morris, I. V. Sazanovich, J. A. G. Williams and J. A. Weinstein, *Chem. Sci.*, 2014, **5**, 879–886.
5 E. Baggaley, J. A. Weinstein and J. A. G. Williams, *Struct. Bonding*, 2015, **165**, 205–256.
6 A. Colombo, F. Fiorini, D. Septiadi, C. Dragonetti, F. Nisic, A. Valore, D. Roberto, M. Mauro and L. De Cola, *Dalton Trans.*, 2015, **44**, 8478–8487.
7 V. W.-W. Yam and A. S.-Y. Law, *Coord. Chem. Rev.*, 2020, **414**, 213298.
8 A. S.-Y. Law, L. C.-C. Lee, K. K.-W. Lo and V. W.-W. Yam, *J. Am. Chem. Soc.*, 2021, **143**, 5396–5405.
9 W. Sotoyama, T. Satoh, N. Sawatari and H. Inoue, *Appl. Phys. Lett.*, 2005, **86**, 153505–153507.
10 M. Cocchi, D. Virgili, V. Fattori, D. L. Rochester and J. A. G. Williams, *Adv. Funct. Mater.*, 2007, **17**, 285–289.
11 X. Yang, Z. Wang, S. Madakuni, J. Li and G. E. Jabbour, *Adv. Mater.*, 2008, **20**, 2405–2409.
12 W. Y. Wong and C. L. Ho, *Chem. Soc. Rev.*, 2009, **253**, 1709–1758.
13 C. M. Che, C. C. Kwok, S. W. Lai, A. F. Rausch, W. J. Finkenzeller, N. Y. Zhu and H. Yersin, *Chem. – Eur. J.*, 2010, **16**, 233–247.
14 J. Kalinowski, V. Fattori, M. Cocchi and J. A. G. Williams, *Coord. Chem. Rev.*, 2011, **255**, 2401–2425.
15 E. Rossi, L. Murphy, P. L. Brothwood, A. Colombo, C. Dragonetti, D. Roberto, R. Ugo, M. Cocchi and J. A. G. Williams, *J. Mater. Chem.*, 2011, **21**, 15501–15510.
16 L. F. Gildea and J. A. G. Williams, Iridium and platinum complexes for OLEDs, in *Organic Light-Emitting Diodes: Materials, Devices and Applications*, ed. A. Buckley, Woodhead, Cambridge, 2013.
17 F. Nisic, A. Colombo, C. Dragonetti, D. Roberto, A. Valore, J. M. Malicka, M. Cocchi, G. R. Freeman and J. A. G. Williams, *J. Mater. Chem. C*, 2014, **2**, 1791–1800.
18 C. Cebrian and M. Mauro, *Beilstein J. Org. Chem.*, 2018, **14**, 1459–1481.
19 X. Yang, H. Guo, X. Xu, Y. Sun, G. Zhou, W. Ma and Z. Wu, *Adv. Sci.*, 2019, **6**, 1801930.
20 W.-C. Chen, C. Sukpattanacharoen, W.-H. Chan, C.-C. Huang, H.-F. Hsu, D. Shen, W.-Y. Hung, N. Kungwan, D. Escudero, C.-S. Lee and Y. Chi, *Adv. Funct. Mater.*, 2020, **30**, 2002494.
21 A. Haque, H. El Moll, K. M. Alenezi, M. S. Khan and W. Y. Wong, *Materials*, 2021, **14**, 4236–4261.
22 A. S.-Y. Law, M. C.-L. Yeung and V. W.-W. Yam, *ACS Appl. Mater. Interfaces*, 2017, **9**, 41143–41150.
23 Y. Y. Ning, G. Q. Jin, M. X. Wang, S. Gao and J. L. Zhang, *Curr. Opin. Chem. Biol.*, 2022, **66**, 102097–102107.
24 E. Rossi, A. Colombo, C. Dragonetti, S. Righetto, D. Roberto, R. Ugo, A. Valore, J. A. G. Williams, M. G. Lobello, F. De Angelis, S. Fantacci, I. Ledoux-Rak, A. Singh and J. Zyss, *Chem. – Eur. J.*, 2013, **19**, 9875–9883.
25 A. Colombo, C. Dragonetti, D. Marinotto, S. Righetto, D. Roberto, S. Tavazzi, M. Escadeillas, V. Guerchais, H. Le Bozec, A. Boucekkine and C. Latouche, *Organometallics*, 2013, **32**, 3890–3894.
26 H. Zhao, E. Garoni, T. Roisnel, A. Colombo, C. Dragonetti, D. Marinotto, S. Righetto, D. Roberto, D. Jacquemin, J. Boixel and V. Guerchais, *Inorg. Chem.*, 2018, **57**(12), 7051–7063.
27 S. Attar, F. Artizzu, L. Marchik, D. Espa, L. Pilia, M. F. Casula, A. Serpe, M. Pizzotti, A. Orbelli-Biroli and P. Deplano, *Chem. – Eur. J.*, 2018, **24**, 10503–10512.
28 A. Colombo, C. Dragonetti, V. Guerchais and D. Roberto, *Coord. Chem. Rev.*, 2021, **446**, 214113–213133.
29 H. Yersin, A. F. Rausch, R. Czerwieniec, T. Hofbeck and T. Fischer, *Coord. Chem. Rev.*, 2011, **255**, 2622–2652.
30 P. T. Chou, Y. Chi, M. W. Chung and C. C. Lin, *Coord. Chem. Rev.*, 2011, **255**, 2653–2665.
31 E. A. Wood, L. F. Gildea, D. S. Yufit and J. A. G. Williams, *Polyhedron*, 2021, **207**, 115401–115409.
32 M. A. Baldo, D. F. O'Brien, Y. You, A. Shoustikov, S. Sibley, M. E. Thompson and S. R. Forest, *Nature*, 1998, **395**, 151.
33 M. A. Baldo, D. F. O'Brien, M. E. Thompson and S. R. Forrest, *Phys. Rev. B: Condens. Matter Mater. Phys.*, 1999, **60**, 14422.
34 H. Yersin, *Top. Curr. Chem.*, 2004, **241**, 1–26.
35 M. Koden, *OLED Displays and Lighting*, John Wiley & Sons, NJ, 2016.
36 D. Ma, in *Handbook of Advanced Lighting Technology*, ed: R. Karlicek, C.-C. Sun, G. Zissis and R. Ma, Springer International Publishing, Cham, 2016, pp. 1–34.
37 V. Adamovich, J. Brooks, A. Tamayo, A. M. Alexander, P. I. Djurovich, B. W. D'Andrade, C. Adachi, S. R. Forrest and M. E. Thompson, *New J. Chem.*, 2002, **26**, 1171–1178.
38 M. Cocchi, J. Kalinowski, V. Fattori, J. A. G. Williams and L. Murphy, *Appl. Phys. Lett.*, 2009, **94**, 073309–073311.
39 W. Mroz, C. Botta, U. Giovanella, E. Rossi, A. Colombo, C. Dragonetti, D. Roberto, R. Ugo, A. Valore and J. A. G. Williams, *J. Mater. Chem.*, 2011, **21**, 8653–8661.
40 E. Rossi, A. Colombo, C. Dragonetti, D. Roberto, F. Demartin, M. Cocchi, P. Brulatti, V. Fattori and J. A. G. Williams, *Chem. Commun.*, 2012, **48**, 3182–3184.

41 P. Brulatti, V. Fattori, S. Muzzioli, S. Stagni, P. P. Mazzeo, D. Braga, L. Maini, S. Milita and M. Cocchi, *J. Mater. Chem. C*, 2013, **1**, 1823–1831.
42 Y. C. Wei, S. F. Wang, Y. Hu, L. S. Liao, D. G. Chen, K. H. Chang, C. W. Wang, S. H. Liu, W. H. Chan, J. L. Liao, W. Y. Hung, T. H. Wang, P. T. Chen, H. Hsu, F. Y. Chi and P. T. Chou, *Nat. Photonics*, 2020, **14**, 570–577.
43 P. P. Ghoroghchian, P. R. Frail, K. Susumu, D. Blessington, A. K. Brannan, F. S. Bates, B. Chance, D. A. Hammer and M. J. Therien, *Proc. Natl. Acad. Sci. U. S. A.*, 2005, **102**, 2922–2927.
44 L. Yuan, W. Lin, S. Zhao, W. Gao, B. Chen, L. He and S. Zhu, *J. Am. Chem. Soc.*, 2012, **134**, 13510–13523.
45 G. Qian and Z. Y. Wang, *Chem. – Asian J.*, 2010, **5**, 1006–1029.
46 J. V. Caspar and T. J. Meyer, *J. Phys. Chem.*, 1983, **87**, 952–957.
47 J. A. G. Williams, A. Beeby, S. Davies, J. A. Weinstein and C. Wilson, *Inorg. Chem.*, 2003, **42**, 8609–8611.
48 S. J. Farley, D. L. Rochester, A. L. Thompson, J. A. K. Howard and J. A. G. Williams, *Inorg. Chem.*, 2005, **44**, 9690–9703.
49 J. A. G. Williams, *Chem. Soc. Rev.*, 2009, **38**, 1783–1801.
50 A. F. Rausch, L. Murphy, J. A. G. Williams and H. Yersin, *Inorg. Chem.*, 2012, **51**, 312–319.
51 A. Rodrigue-Witchel, D. L. Rochester, S. B. Zhao, K. B. Lavelle, J. A. G. Williams, S. Wang, W. B. Connick and C. Reber, *Polyhedron*, 2016, **108**, 151–155.
52 C. Dragonetti, F. Fagnani, D. Marinotto, A. Di Biase, D. Roberto, M. Cocchi, S. Fantacci and A. Colombo, *J. Mater. Chem. C*, 2020, **8**, 7873–7881.
53 D. L. Rochester, S. Develay, S. Zális and J. A. G. Williams, *Dalton Trans.*, 2009, 1728–1741.
54 M. Cocchi, J. Kalinowski, L. Murphy, J. A. G. Williams and V. Fattori, *Org. Electron.*, 2010, **11**, 388–396.
55 W. Sotoyama, T. Satoh, H. Sato, A. Matsuura and N. Sawatari, *J. Phys. Chem. A*, 2005, **109**, 9760–9766.
56 L. Murphy, P. Brulatti, V. Fattori, M. Cocchi and J. A. G. Williams, *Chem. Commun.*, 2012, **48**, 5817–5819.
57 F. Fagnani, A. Colombo, C. Dragonetti, D. Roberto and D. Marinotto, *Inorg. Chim. Acta*, 2022, **532**, 120744.
58 C. Hierlinger, D. B. Cordes, A. M. Z. Slawin, A. Colombo, C. Dragonetti, S. Righetto, D. Roberto, D. Jacquemin, E. Zysman-Colman and V. Guerchais, *Dalton Trans.*, 2018, **47**, 8292.
59 J. Kalinowski, M. Cocchi, L. Murphy, J. A. G. Williams and V. Fattori, *Chem. Phys.*, 2010, **378**, 47–57.
60 J. Kalinowski, W. Stampor, J. Szmytkowski, D. Virgili, M. Cocchi, V. Fattori and C. Sabatini, *Phys. Rev. B*, 2006, **74**, 85316.
61 M. Cocchi, D. Virgili, V. Fattori, J. A. G. Williams and J. Kalinowski, *Appl. Phys. Lett.*, 2007, **90**, 023506.
62 U. Balijapalli, R. Nagata, N. Yamada, H. Nakanotani, M. Tanaka, A. D'Aléo, V. Placide, M. Mamada, Y. Tsuchiya and C. Adachi, *Angew. Chem., Int. Ed.*, 2021, **60**, 8477–8482.
63 Y. Zhang, J. Miao, J. Xiong, K. Li and C. Yang, *Angew. Chem.*, 2022, **61**, e202113718.
64 L. Cao, J. Li, Z.-Q. Zhu, L. Huang and J. Li, *ACS Appl. Mater. Interfaces*, 2021, **13**, 60261–60268.
65 M. Z. Shafikov, P. Pander, A. V. Zaytsev, R. Daniels, R. Martinscroft, F. B. Dias, J. A. G. Williams and V. N. Kozhevnikov, *J. Mater. Chem. C*, 2021, **9**, 127–135.